JOURNAL OF MATERIALS SCIENCE **38** (2003) 3861 – 3870

Reactive processing of nickel-aluminide intermetallic compounds

H. X. ZHU*, R. ABBASCHIAN
Department of Materials Science and Engineering, University of Florida,
Gainesville, FL 32611, USA
E-mail: hzhu@mail.mse.ufl.edu

NiAl have been fabricated by reactive sintering compacts of ball-milled powder mixtures containing Ni and Al. The reaction mechanism, as well as phase and microstructural development, were investigated by analyzing compacts quenched from different temperatures during reactive hot compaction. It was found that the reaction process was strongly affected by pressure, heating rates, heat loss from the sample to the environment. The application of 50 MPa prior to the reaction resulted in the intermetallic-formation reaction initiating at a temperature (480°C) much lower than that (∼550°C) when no pressure was applied. At high heating rate (50°C/min), when the heat loss is small, the formation of NiAl occurs rapidly via combustion reaction. On the other hand, if the heat loss is significant as in slow heating rate (10°C/min), the reaction process is controlled by solid-state diffusion. The phase formation sequence for the slow solid-state reaction was determined to be: $NiAl_3 \rightarrow Ni_2Al_3 \rightarrow NiAl \rightarrow NiAl$ (Al-rich) $+ Ni_3Al \rightarrow NiAl$. © *2003 Kluwer Academic Publishers*

1. Introduction

Reactive synthesis of NiAl and Ni_3Al intermetallic compounds has received much attention in recent years for obtaining dense intermetallic compounds from elemental Ni and Al powders. Several reactive processing methods such as combustion synthesis [1–4], reactive hot compaction [5], reactive hot isostatic press [6, 7] and reactive infiltration processing [8–11] have been successfully utilized to synthesize the intermetallic compounds. Plazanet and Nardou [4] studied the reaction process during sintering of NiAl via combustion synthesis. They found that at heating rates higher than 5°C/min, the combustion could be ignited by preheating the sample at 538°C. The combustion could not be ignited with heating rates lower than 5°C/min. In this case, the intermediate $NiAl_3$ and Ni_2Al_3 phases formed during heating the Ni-Al powder compacts before the formation of NiAl phase at 1100°C. The final products in both cases for the pressureless reactive sintering of NiAl were found to be porous due to high volume reduction. In order to achieve higher product densities, reactive hot compaction (RHC) [5] and reactive hot isotropic press (RHIP) [6] have been developed to produce NiAl and its composites. It was found that fully densified NiAl could be achieved if process was appropriately controlled such that adequate mass flow takes place to feed shrinkage volume. The microstructural evolution during reactive hot compaction of Ni + Al + prealloyed NiAl powder mixtures at a high heating rate of 100°C/min has been investigated by Doty [5]. It was found that the reaction could not proceed to completion when the temperature reached the ignition temperature (about 485°C) due to the significant cooling imposed on the specimen by contact with the graphite die. The quenched specimen had a multi-phase microstructure containing Ni, supersaturated NiAl (possibly $NiAl_3$ according to the microprobe analysis), Ni_3Al and prealloyed NiAl. After about 30 min. sintering at 1250°C, the uniform structure with only NiAl was achieved.

More recently, solid state reaction synthesis of NiAl from fully dense elemental Ni and Al powder blends has been developed by Farber *et al.* [12, 13]. The method involves high pressure (up to 250 MPa) consolidation of very fine elemental powder blends to full density followed by controlled solid state reactive hot press at a relatively low heating rate (20°C/min). No measurable self-heating of the samples was observed in the hot press. It was found that after 10 min exposure at 550°C, all the elemental Al was consumed in the formation of the Al-rich $NiAl_3$ and Ni_2Al_3 aluminides. It was believed that both slow heating and effective heat transfer from the sample to the massive pressure die prevented the reaction from becoming self-sustaining and allowed the reaction to remain solid state diffusion-controlled.

In this paper, the effects of pressure, heating rate and heat exchange conditions between the sample and its surroundings on the reaction process during the

---

*Author to whom all correspondence should be addressed.

0022–2461 © *2003 Kluwer Academic Publishers*

reactive hot compaction of Ni + Al powders were investigated. The reaction mechanism, as well as phase and microstructural development, was studied by quenching the compacts from different temperatures during hot press.

2. Experimental procedure

Aluminum and nickel powders, with the average particle sizes in the range of 3.0–4.5 μm and 2.0–3.0 μm, respectively, were blended in 1 to 1 molar ratio for at least 10 h using a ball mill. About 14 g of the mixed powder was put into in a boron nitride coated, graphite foil lined graphite die with a diameter of 38.4 mm, and cold compacted at 50 MPa. The compacts were then vacuum hot pressed to temperatures ranging from 400 to 1200°C with heating rates of 10 and 50°C/min and a pressure of 50 MPa. The sample was then quenched at given temperatures during heating by turning off the induction power. The temperature changes of the samples during vacuum hot press were measured by a K-type (NiCr-NiAl) thermocouple inserted near the center of the samples. An Al_2O_3 powder compact was used as the standard for the measurement. The temperature difference of the sample and the standard was also measured during vacuum hot press. Three tests were conducted; the first one (mode A) at a heating rate of 10°C/min, the second one at 50°C/min (mode B) and the third one using sample well insulated with Al_2O_3 at a heating rate of 50°C/min (mode C).

The differential thermal analysis (DTA) of the powder mixtures, cold compacted at 50 MPa, was carried out to obtain information about reaction temperatures during the reactive sintering process. As the reactive synthesis techniques are sensitive to the heating rates adopted, the effect of heating rate on the reaction was studied at three different heating rates, 5, 10 and 50°C/min, with the argon flow of 100 ml/min. Phase identification in the quenched samples was performed employing X-ray diffraction (XRD) with a Cu X-ray tube (($\lambda_{\mathrm{Cu\,K}_\alpha} = 0.154056$ nm) operating at 40 kV and 20 mA. Scanning was performed in a step mode with a 0.02° step and a 1s exposure in a 10–90° diffraction angle range. Microstructures of the samples and chemical composition of different phases were studied employing a scanning electron microscope (SEM) JSM-6400 with an energy dispersive spectrometer (EDS). Quantitative EDS analysis was based on K_α analytical lines from the spectra acquired at the 15 kV accelerating voltage. Aluminum was used as a standard, and ZAF correction was performed.

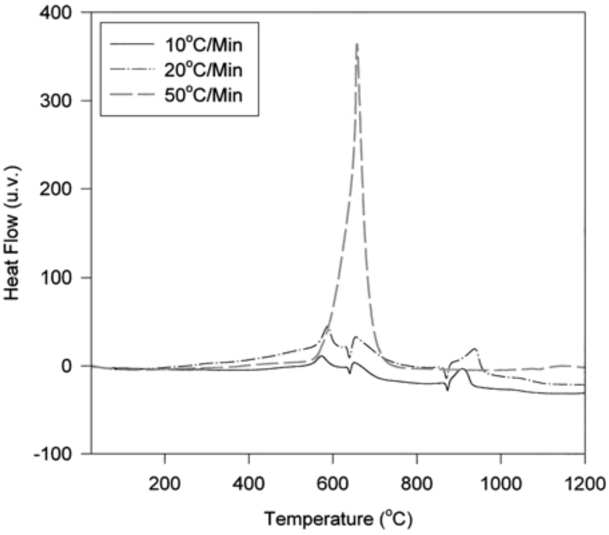

Figure 1 DTA curves of Ni + Al powder compacts at heating rates of 10, 20 and 50°C/min.

3. Results

3.1. Differential thermal analysis (DTA)

DTA has been performed on the green compacts of Ni + Al powder mixtures using heating rates of 5, 10, 20 and 50°C/min. The DTA curves in Fig. 1 indicate the occurrence of several exothermic and endothermic reactions at temperatures summarized in Table I. Since the starting temperatures for the exotherms are not well defined, the temperatures corresponding to the maximum points in the curves are reported for the occurrence of the exothermic reactions. The starting temperatures for the endotherms, on the other hand, are better defined and are also reported in Table I. For Ni + Al powder compacts, three exothermic peaks and two endothermic peaks were observed at lower heating rates (5, 10 and 20°C/min), while only one strongly exothermic peak was detected at higher heating rate (50°C/min), starting at 550°C (Fig. 1). It can be seen that the temperatures for the exothermic peaks increased with increasing heating rates. However, the heating rate did not have appreciable effect on the endotherm temperatures.

The temperature-time curve and temperature difference of the sample and the standard (Al_2O_3) during

TABLE I Temperatures corresponding to the exothermic and endothermic events in the Ni + Al powder compacts obtained from DTA at heating rates of 5, 10, 20 and 50°C/min

	5°C/min		10°C/min		20°C/min		50°C/min	
Heating rate samples	Exotherm (°C)	Endotherm (°C)	Exotherm (°C)	Endotherm (°C)	Exotherm (°C)	Endotherm (°C)	Exotherm (°C)	Endotherm (°C)
Ni + Al	557		572		587		—	
		642		640		639		—
	648		649		653		657	
		863		873		870		—
	892		908		937		—	

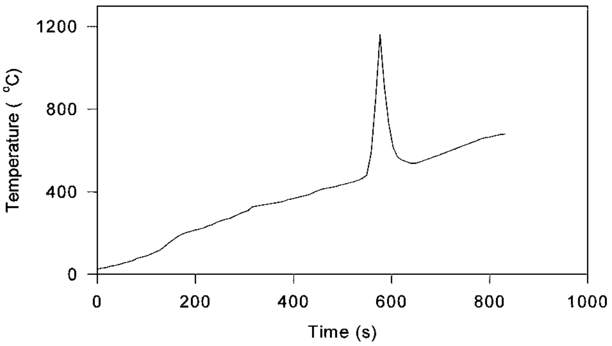

Figure 2 The sample temperature vs. time curve for the alumina-insulated Ni + Al powder compacts during RHC at a heating rate of 50°C/min.

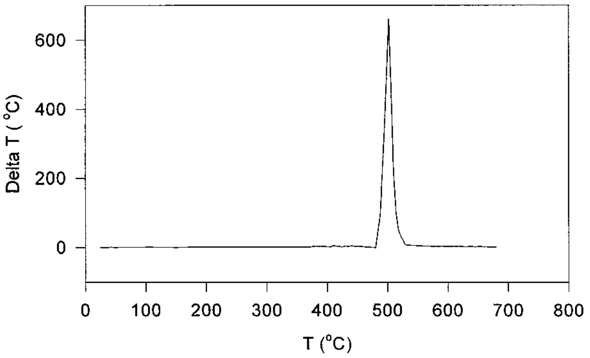

Figure 3 The temperature difference ($\Delta T = T_1 - T$) vs. T curve for the insulated Ni + Al powder compacts during RHC at a heating rate of 50°C/min (T_1, T are the temperatures for the sample and the Al_2O_3 standard, respectively).

RHC, measured by using K type thermocouple inserted inside the sample and the standard, are shown in Figs 2 and 3, respectively. It can be seen that for the well-insulated sample (mode C), the ignition temperature of about 480°C is very close to 485°C estimated by Doty [5] at a heating rate of 100°C/min under similar conditions. The application of pressure in the hot press reduced the ignition temperature from 550°C to 480°C. The maximum temperature was measured as about 1200°C, which is much lower than the theoretical temperature, 1638°C, predicted by the thermodynamic calculation [14].

The ΔT vs. T curves for the other two Ni + Al samples at the normal hot press conditions at heating rates of 10 and 50°C/min are shown in Fig. 4 (mode A and B). Although only one peak was observed for the sample at a heating rate of 50°C/min, the temperature increase of the sample was very limited, at a range of about 20°C, in contrast to about 700°C for the insulated sample shown in Fig. 3. At a heating rate of 10°C/min, only one very weak peak was observed. Unlike the well-insulated samples (Fig. 3) which reacted in an explosive manner when heated above 480°C, no measurable self-heating of the samples was observed in the hot press at a slow heating rate of 10°C/min (Fig. 4). As discussed later, both slow heating and effective heat transfer from the sample to the massive graphite mold prevented the reaction from becoming self-sustaining and allowed the reaction to remain solid state diffusion-controlled.

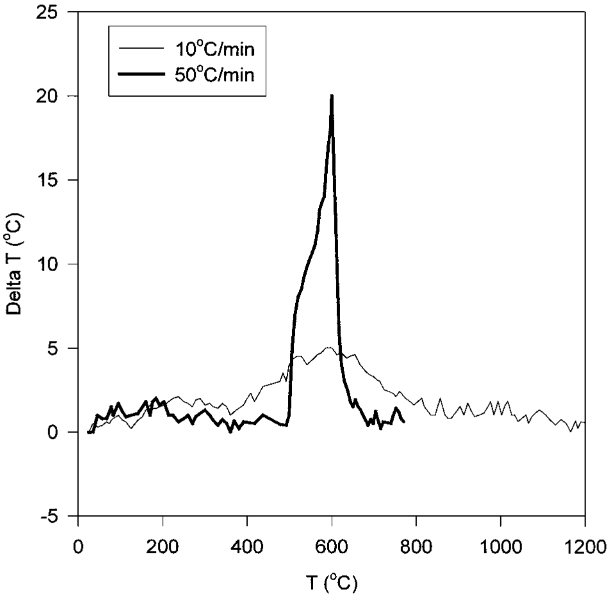

Figure 4 The temperature difference ($\Delta T = T_1 - T$) vs. T curve for the Ni + Al powder compacts during RHC at heating rates of 10 and 50°C/min without insulation (normal RHC).

3.2. X-ray diffraction analysis (XRD)

The evolution of the phases during RHC was investigated by halting the heating at different temperatures. The XRD patterns of the samples heated to 600°C at a rate of 50°C/min with (mode C) and without insulation (mode B) are shown in Figs 5 and 6 respectively. It can be seen that for the well-insulated samples, the final products only consist of NiAl phase (Fig. 5), while

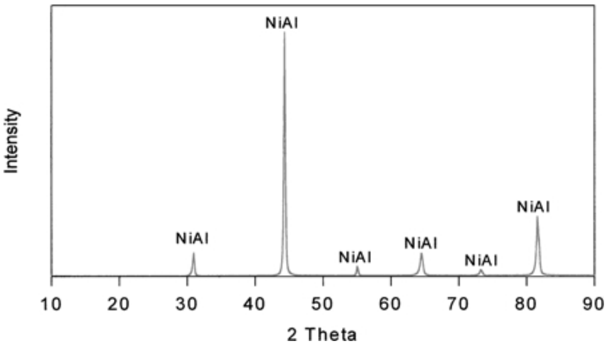

Figure 5 XRD patterns of the final product formed when the insulated Ni + Al powder mixtures were reactive hot pressed to 600°C at a heating rate of 50°C/min.

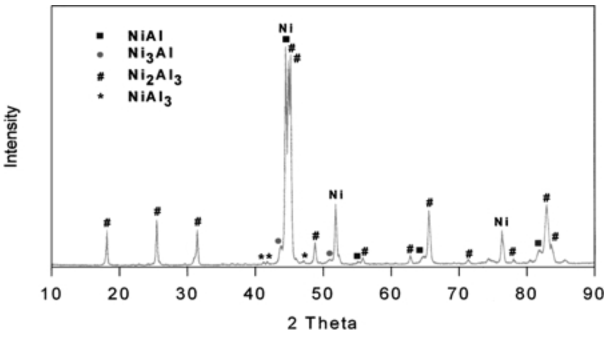

Figure 6 XRD patterns of the final product formed when the Ni + Al powder mixtures were reactive hot pressed to 600°C at a heating rate of 50°C/min without insulation.

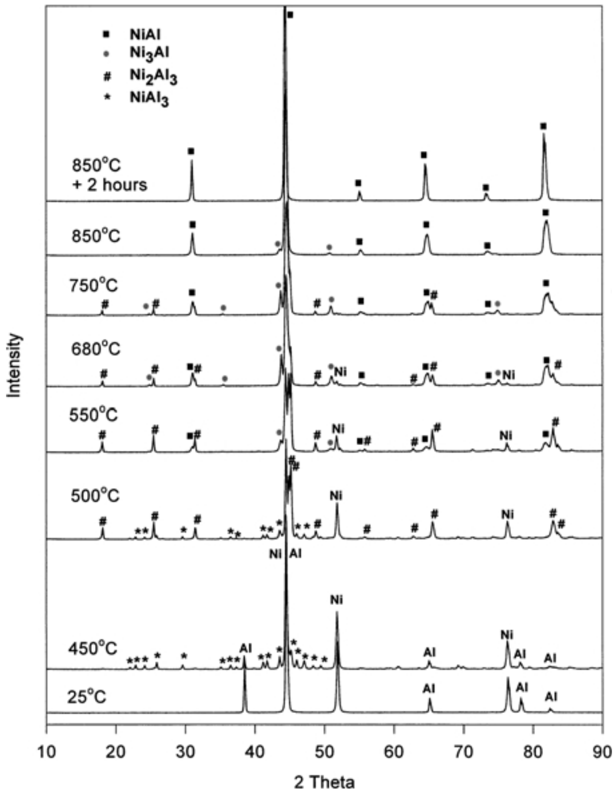

Figure 7 XRD patterns of the intermediate products formed upon heating to the temperature indicated during reactive hot compaction of Ni + Al powder mixtures at a heating rate of 10°C/min without insulation.

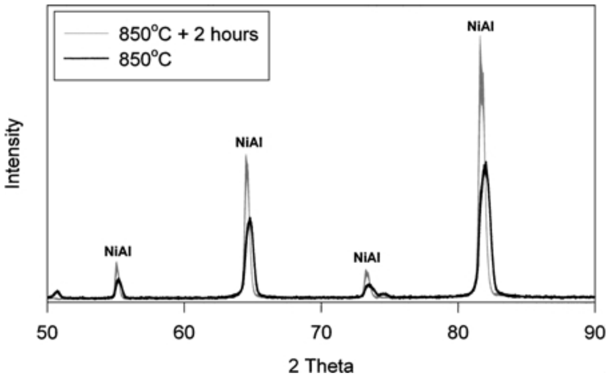

Figure 8 XRD patterns of the reactive hot compactioned Ni + Al powder compacts heated to 850°C and held for 0 and 2 h at a heating rate of 10°C/min, showing the NiAl peak shift.

for the other samples, the final products are composed of Ni_2Al_3, NiAl, Ni_3Al and Ni multi-phases (Fig. 6). The results indicated that the heat exchange condition controlled the completion of combustion reaction from Ni + Al to NiAl, and that heat loss resulting from the heat exchange between the samples and graphite mold may prevent the combustion reaction from becoming self-sustaining.

XRD diagrams for the reactive hot pressed powder mixtures from room temperature to 850°C at a heating rate of 10°C/min (mode A) are shown in Fig. 7. It can be seen that after milling, X-ray diffraction patterns do not show any peaks which are different from those of Al and Ni. At a temperature less than 400°C, no new phases were detected either. As the temperature is raised to about 450°C, peaks related to the formation of $NiAl_3$ appear, while the Al peaks weaken. When the temperature reaches 500°C, the Al peaks are completely replaced by those corresponding to Ni_2Al_3, and the $NiAl_3$ peaks weaken. At 550°C, the $NiAl_3$ peaks disappear and the peaks corresponding to NiAl and Ni_3Al appear. From 550°C to 680°C, the four phases Ni_2Al_3, NiAl, Ni_3Al and Ni co-exist, however, NiAl and Ni_3Al grow at the expense of Ni_2Al_3 and Ni. As the temperature is raised to 750°C, the Ni peaks disappear. When the temperature reaches 850°C, NiAl becomes the major phase, only minor Ni_3Al exists and the Ni_2Al_3 peaks disappear. After about two hours at 850°C, the reaction is complete and the samples only consist of NiAl. The peaks of NiAl in all the XRD patterns of the samples halted at different temperature (550–850°C) were slightly shifted towards higher diffraction angles in comparison to those of the NiAl after two-hour holding at 850°C (Fig. 8), indicating a smaller lattice parameter than that of stoichiometric NiAl. It has been shown that both Ni-rich and Al-rich compounds have lattice parameters smaller than that of the stoichiometric NiAl [3]. Therefore, it can be suggested that after heating to 850°C via RHC, the synthesized sample consist of a mixture of the hypo- and hyperstoichiometric NiAl. This will be confirmed by the EDS analysis presented later.

3.3. Microstructural development

Microstructures of the hot pressed powder compacts heated to different temperatures from 400°C to 1200°C at a heating rate of 10°C/min are shown in Fig. 9. Intermediate phases such as $NiAl_3$, Ni_2Al_3 and $Ni_3Al$are produced during reactive hot press depending on the temperature. At 400°C, no other phases other than Ni (seen as gray in the micrograph) and Al (black) were detected by EDS. The spherical Al powers deformed due to the application of 50 MPa pressure, resulting in a continuous Al network surrounding the Ni powders. As temperature increases, $NiAl_3$ forms at the interface between Ni and Al. At 450°C, a large amount of $NiAl_3$ is produced with only a small amount of Al remaining (Fig. 4b, c). At 500°C, Ni_2Al_3 grows at the expense of $NiAl_3$ and Ni and becomes the main phase in the sample. When the samples were heated to 550°C, both NiAl and Ni_3Al were detected at the interface between Ni and Ni_2Al_3. At 680°C, NiAl became the dominant phase, but the four-phase Ni/Ni_3Al/NiAl/Ni_2Al_3 structures co-existed over a large temperature range (550–750°C). At 680°C, NiAl was determined to be Al-rich (53at.%Al - 47at.%Ni) by EDS.

Only a two-phase NiAl/Ni_3Al structure was observed when the samples were heated to 850°C (Fig. 9h). A Ni-rich NiAl was detected at the interface between NiAl and Ni_3Al after heating in the range of 750 and 850°C (Fig. 9g, h). After a two-hour anneal at 850°C (or continuing to heat to 1000°C), no additional reaction was detected, and the sample contained a uniform NiAl structure with small amount of Al_2O_3 plus some porosity (Fig. 9i). Finally, after two hours at 1200°C, a near fully dense NiAl was achieved (Fig. 9j).

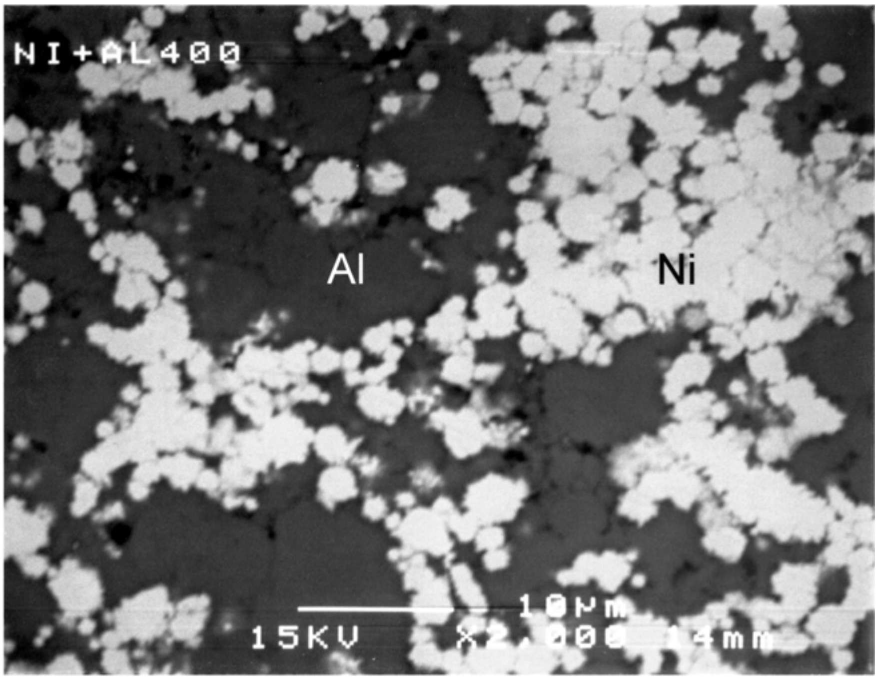

(a)

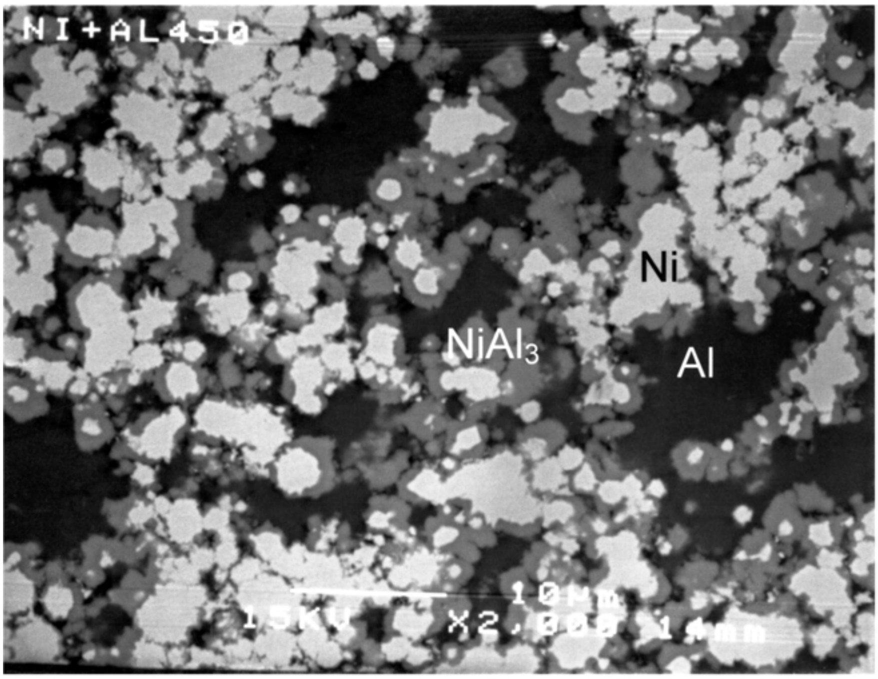

(b)

Figure 9 SEM micrographs (BSE mode) of the Ni + Al powder compacts heated to (a) 400°C, (b) 450°, (c) 450°C (high magnification), (d) 500°C, (e) 600°C, (f) 680°C, (g) 750°C, (h) 850°C, (i) 850°C holding two hours, and (j) (SE mode) 1200°C holding two hours during RHC at a heating rate of 10°C/min. *(Continued)*

4. Discussions

The highly exthothermic nature of the powder mixture of Ni + Al has been utilized for reactive sintering of NiAl. Based on the Ni-Al phase diagram [15], the binary system exhibits two solid solutions and five stable intermetallic compounds, $NiAl_3$, Ni_2Al_3, NiAl, Ni_5Al_3 and Ni_3Al, four of which have been detected in this study. The reaction mechanism and phase formation sequences of the Ni-Al powder compacts under pressureless sintering (DTA) and reactive hot compaction will be discussed in detail below.

The evolution of the phases and the reaction paths during pressureless sintering of the powder compacts may be discerned from the exothermic and endothermic peaks in the DTA curves of Fig. 1. At high heating rate (50°C/min), only one exothermic peak was observed for the Ni-Al powder mixtures suggesting that the formation of NiAl was achieved in one-step as supported by previous XRD analysis [5]. However, several exothermic and endothermic peaks were observed at lower heating rates (5–20°C/min). A comparison of the temperatures for the endotherms and the melting points of the various possible phases in the Ni-Al phase

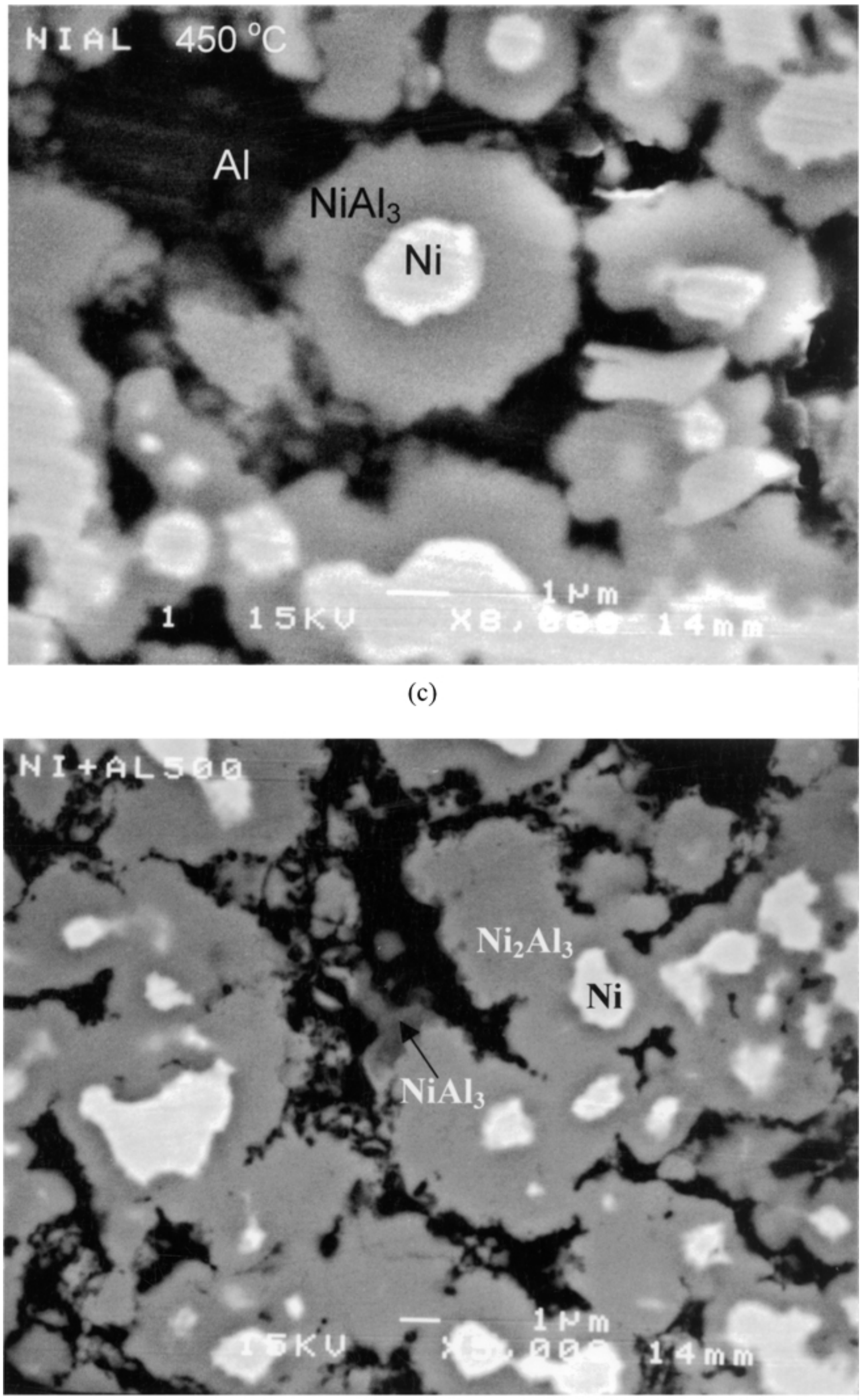

(c)

(d)

Figure 9 (Continued).

diagram [15] suggests that the endotherm at ~640°C corresponds to the eutectic point of Al and $NiAl_3$, while the endotherm at ~860°C corresponds to the melting points of $NiAl_3$. Based on the appearance of these endotherms, the first exothermic peak may be assigned to the formation of $NiAl_3$ while the second and the third peaks may be due to the formation of Ni_2Al_3 and NiAl, respectively. Therefore, the formation sequence of the phases during pressureless sintering of Ni + Al powder compacts may be explained as follows. Al initially reacts with elemental nickel to form $NiAl_3$, and this reaction occurs at the temperature corresponding to the first exothermic peak. Upon further heating, a portion of the $NiAl_3$ forms an eutectic with Al and melts at 640°C (first endothermic reaction). $NiAl_3$ reacts with Ni to form Ni_2Al_3 at the second exothermic peak. The 660°C endotherm (Al melting) is not distinguishable since the second exothermic peak occurs almost at the same temperature. The unreacted $NiAl_3$ melts upon reaching its melting point (the 860°C endotherm). Finally, the $NiAl_3$ and Ni_2Al_3 react with Ni to form NiAl (the third exotherm). Thus the formation sequence of the various phases during pressureless sintering of Ni-Al powders is possibly $NiAl_3 \rightarrow Ni_2Al_3 \rightarrow NiAl$. The

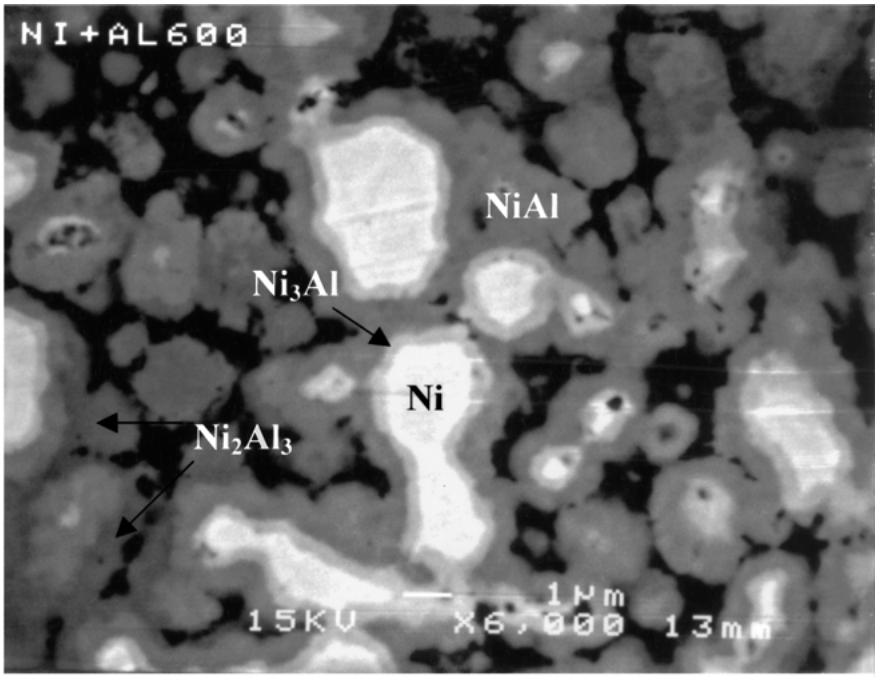

(e)

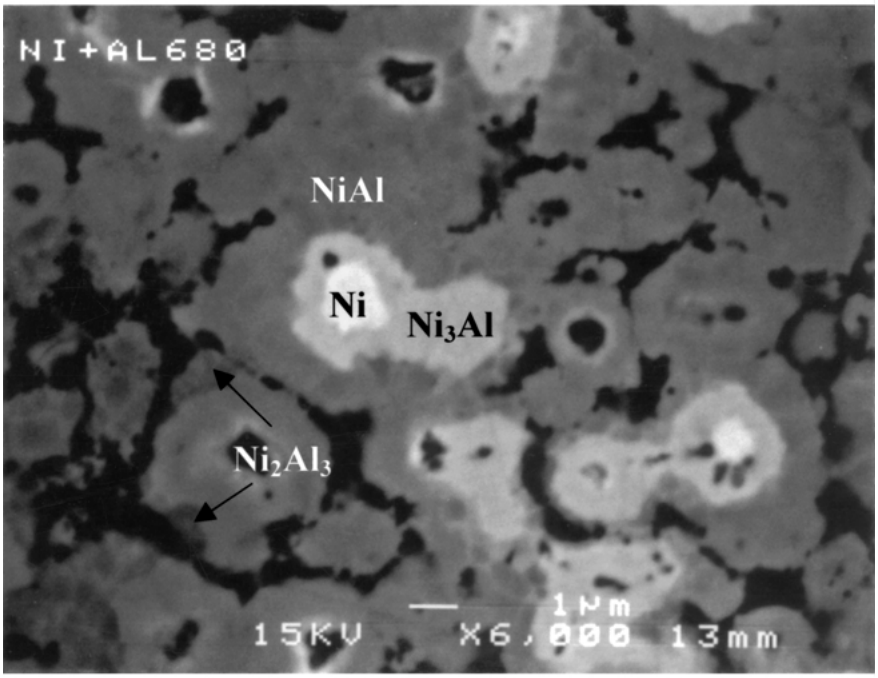

(f)

Figure 9 (Continued).

studies of diffusion couples of Al and Ni [16–18] and the predictions of the effective heat of formation model of Pretorius *et al.* [19] on the thin film compound phase formation also indicate a similar sequence of formation. The DTA results of Dyer and Munir [20] and Rein *et al.* [21] also showed three exothermic peaks at heating rates of lower than 50 K/min in the case of Ni-Al multilayers and Ni-Al powder mixtures. They also attributed the peaks to the formation of $NiAl_3$, Ni_2Al_3 and NiAl.

The reaction process under pressure via RHC was found different from that via pressureless sintering. The temperature-time curve (Fig. 2) for the insulated sample at a heating rate of 50°C/min revealed a single exotherm near 480°C resulting in a steep temperature increase. XRD analysis of the specimens (Fig. 5) showed that the formation of NiAl from Ni + Al powders had gone to completion. As such, the application of 50 MPa resulted in the intermetallic-formation reaction initiation at a temperature much lower than that when no pressure was applied. This is apparently related to the increased contact between the powders caused by damage to the oxide scale which provides more reaction nucleation sites and thus, the autocatalytic effect of the heat of formation

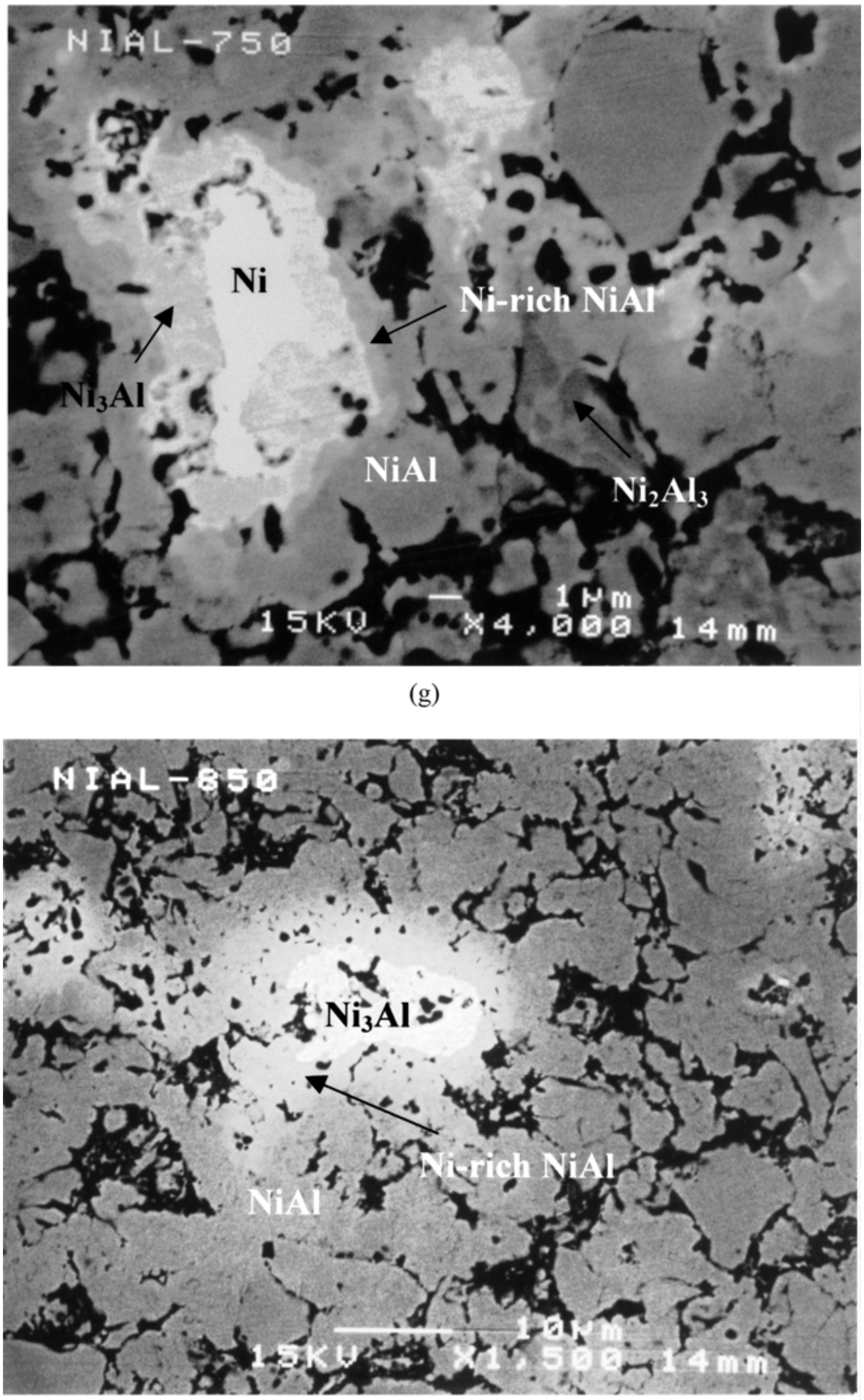

(g)

(h)

Figure 9 (Continued).

begins at a lower temperature. The thermodynamic analysis [14] indicated that, during reactive sintering of Ni + Al powders, the maximum temperature T_{ad} would reach 1911 K and the molten NiAl would possibly form. However, the maximum temperature of around 1473 K indicates that considerable amounts of heat was lost during RHC. If no insulation materials are used, a multi-phase $NiAl_3/Ni_2Al_3/NiAl/Ni$ structure (Fig. 6) was formed when the sample was heated to 600°C at the same heating rate during RHC. These results show that the significant heat loss due to heat conduction between the powder compacts and the graphite mold can prevent the reaction from becoming self-sustaining. Similar results was also reported by Nishimura and Liu [22] during reactive processing of Ni_3Al by using 3Ni + Al powder mixtures. It was shown that the heat flow strongly affected the reaction process, and an efficient heat removal by using alumina blocks could prevent the reaction from becoming self-sustaining, in which case only $NiAl_3$ and Ni_2Al_3 phases formed.

On the other hand, at a lower heating rate of 10°C/min, no obvious self-heating was observed during RHC of the compacts (Fig. 4). The XRD and

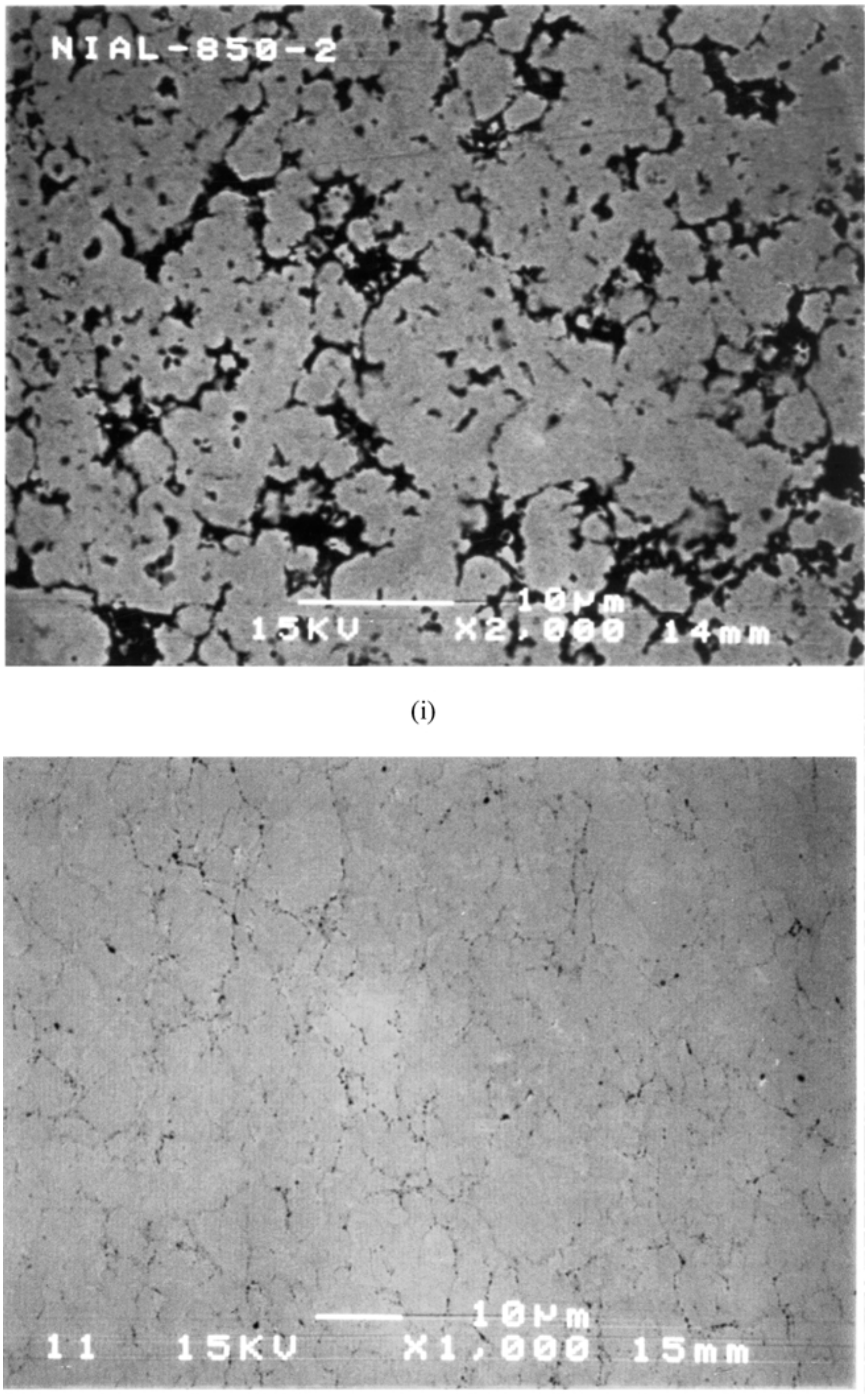

(i)

(j)

Figure 9 (Continued).

EDS analysis indicated that the first phase formed was $NiAl_3$ at a temperature between 400°C and 450°C, followed by the formation of Ni_2Al_3 at a temperature between 450°C and 500°C. At 500°C, no Al was detected by XRD indicating that Al was completely consumed before melting. As the temperature was raised, NiAl and Ni_3Al formed and grew at the expense of Ni and Ni_2Al_3. The results confirm the previous deduction of the phase formation sequence by DTA. However, the intermetallic-formation reaction initiated at much lower temperatures than those predicted by DTA. In addition, no liquid phase was detected during RHC of NiAl at the slow heating rate. The phase formation sequence during reactive hot compaction of Ni + Al powders at a slow heating rate agrees well with the published results [16–18, 23–26]. It is generally believed that $NiAl_3$ is the first phase to form between 250 and 320°C in the case of the reactions that occurs in thin-film Ni-Al multilayers. The slightly higher formation temperature (between 400–450°C) for the $NiAl_3$ phase in this research is believed to be due to the existence of Al_2O_3 shells on the surfaces of the aluminum powders, which act as the diffusion barrier. The detailed study of the influence of oxygen impurities on the reaction of Al-Ni couples by Heald and Barrera [27] indicated that oxygen influenced strongly the course of the reaction. Oxygen impurities within the Al layer inhibited the grain boundary reaction channel, while interfacial oxygen strongly inhibited both the initial reaction and the bulk reaction, possibly by the formation of strong Al—O bonds which acted as a diffusion barrier. In the present study, the aluminum and nickel powders were handled in the air, so thin oxide films most likely formed on the powder surfaces. It has been shown that the existence of thicker Al_2O_3 shells in the case when extensively oxidized Al powders are used further delays the $NiAl_3$ formation to higher temperatures (between 450 and 500°C) [14], consistent with the above explanations of the effect of the oxides.

At low temperatures, Al is the fastest diffusing species in the Ni/Al diffusion couples [23–25]. Therefore, $NiAl_3$ grows via the diffusion of Al through the $NiAl_3$ phase to the $NiAl_3$/Ni interface. After the Al and $NiAl_3$ are consumed, the reaction rate decreases so that even after the temperature is raised to 780°C, a four-layer Ni_2Al_3/NiAl/Ni_3Al/Ni structure is still observed. A similar structure was also observed by Faber *et al.* in their studies of the reaction processes in Ni-Al diffusion couples and Ni-Al powders [13, 27]. However, because diffusion distances in fine micron powder blends are short, the synthesis of NiAl can be completed at relatively low temperatures (for example, after two-hour holding at 850°C). Moreover, the reaction process at slow heating rate is believed to be controlled via solid-state diffusion since no liquid phase was detected during heating process in the present study. Based on the above discussions, the phase formation sequence and the reaction temperatures at 10°C/min heating rate can be described as following:

$$\mathrm{Ni} + 3\mathrm{Al} \rightarrow \mathrm{NiAl_3} \quad (400\text{–}450^\circ\mathrm{C}) \quad (1)$$

$$\mathrm{Ni} + \mathrm{NiAl_3} \rightarrow \mathrm{Ni_2Al_3} \quad (450\text{–}500^\circ\mathrm{C}) \quad (2)$$

$$\mathrm{Ni} + \mathrm{Ni_2Al_3} \rightarrow 3\mathrm{NiAl} \quad (500\text{–}550^\circ\mathrm{C}) \quad (3)$$

$$2\mathrm{Ni} + \mathrm{NiAl} \rightarrow \mathrm{Ni_3Al} \quad (550\text{–}850^\circ\mathrm{C}) \quad (4)$$

$$2\mathrm{Ni_2Al_3} + \mathrm{Ni_3Al} \rightarrow 7\mathrm{NiAl} \quad (550\text{–}750^\circ\mathrm{C}) \quad (5)$$

$$\mathrm{NiAl\ (Al\text{-}rich)} + \mathrm{Ni_3Al} \rightarrow \mathrm{NiAl\ \ (Ni\text{-}rich)} \quad (750\text{–}850^\circ\mathrm{C}) \quad (6)$$

$$\mathrm{NiAl\ (Al\text{-}rich)} + \mathrm{NiAl\ (Ni\text{-}rich)} \rightarrow \mathrm{NiAl} \quad (850\text{–}1200^\circ\mathrm{C\ or\ holding\ at\ }850^\circ\mathrm{C}) \quad (7)$$

5. Summary and conclusions

The reactive sintering of NiAl can be achieved via reactive hot compaction of Ni + Al powder mixtures. The reaction process is strongly affected by pressure, heating rates, heat loss from the sample to its surroundings. The application of 50 MPa prior to the reaction resulted in the intermetallic-formation reaction initiating at a temperature (480°C) much lower than that (~550°C) when no pressure was applied. At high heating rate (50°C/min), when the heat loss is small, the formation of NiAl occurs rapidly via combustion reaction. On the other hand, if the heat loss is significant, as in slow heating rate (10°C/min), the reaction process is slow and controlled by solid-state diffusion. The phase formation sequence for the slow solid-state reaction was determined to be: $NiAl_3 \rightarrow Ni_2Al_3 \rightarrow NiAl \rightarrow NiAl$ (Al-rich) + $Ni_3Al \rightarrow NiAl$.

References

1. J. J. MOORE and H. J. FENG, *Progress in Mater. Sci.* **39** (1995) 243.
2. K. MORSI, *Mater. Sci. Engg.* A **299** (2001) 1.
3. D. B. MIRACLE, *Acta Metall. Mater.* **41** (1993) 649.
4. L. PLAZANET and F. NARDOU, *J. Mater. Sci.* **33** (1998) 2129.
5. H. DOTY and R. ABBASCHIAN, *Mater. Sci. Engg.* A **195** (1995) 101.
6. M. MISOILEK and R. M. GERMAN, *ibid.* A **144** (1991) 1.
7. H. X. ZHU and R. ABBASCHIAN, *Composites*: Part B **31** (2000) 383.
8. D. C. DUNAND, J. L. SOMMER and A. MORTENSEN, *Metall. Trans.* **24A** (1993) 2161.
9. C. SAN MARCHI and A. MORTENSEN, *ibid.* **29A** (1998) 2819.
10. D. C. DUNAND, *Mater. Manuf. Processes* **10** (1995) 373.
11. T. A. VENKATESH, C. SAN MARCHI, A. MORTENSEN and D. C. DUNAND, *Mat. Res. Soc. Symp. Proc.* **460** (1997) 737.
12. L. FARBER, L. KLINGER and I. GOTMAN, *Mater. Sci. Eng.* A **254** (1998) 155.
13. L. FARBER, I. GOTMAN, E. Y. GUTMANAS and A. LAWLEY, *Mater. Sci. Eng.* A **244** (1998) 97.
14. H. X. ZHU, PhD Dissertation, University of Florida, 1999.
15. M. F. SINGLETON, P. NASH and J. L. MURRAY, in "Phase Diagrams of Binary Nickel Alloys," edited by P. Nash (ASM International, Metals Park, OH, 1990) Vol. 1, p. 3.
16. M. M. P. JANSSEN and G. D. RIECK, *Thans. TMS-AIME* **239** (1967) 1372.
17. J. C. LIU, J. W. MAYER and J. C. BARBOUR, *J. Appl. Phys.* **64** (1988) 651.
18. *Idem.*, *ibid.* **64** (1988) 656.
19. R. PRETORIUS, T. K. MARAIS and C.C. THERON, *Mater. Sci. Eng.* R **10** (1993) 1.
20. T. S. DYER and Z. A. MUNIR, *Metall, Mater. Trans.* B **26** (1995) 603.
21. R. REIN, W. A. KAYSSER and G. PETZOV, *Advances in Powder Metallurgy* **9** (1992) 395.
22. C. NISHIMURA and C. T. LIU, *Acta Metall. Mater.* **41** (1993) 113.
23. E. MA, M. A. NICOLET and M. NATHAN, *J. Appl. Phys.* **65** (1989) 2703.
24. E. MA, C. V. THOMPSON and L. A. CLEVENGER, *ibid.* **69** (1991) 2211.
25. E. G. COLGAN, M. NASTASI and J. W. MAYER, *ibid.* **58**(11) (1985) 4125.
26. S. M. HEALD and E. V. BARRERA, *J. Mater. Res.* **6** (1991) 935.
27. L. FARBER, I. GOTMAN and E. Y. GUTMANAS, *Mater. Lett.* **34** (1998) 226.

Received 30 May 2002
and accepted 19 June 2003